A frequency resolved atlas of the sky in continuous gravitational waves

Vladimir Dergachev[1, 2, a] and Maria Alessandra Papa[1, 2, 3, b]

[1]*Max Planck Institute for Gravitational Physics (Albert Einstein Institute), Callinstrasse 38, 30167 Hannover, Germany*
[2]*Leibniz Universität Hannover, D-30167 Hannover, Germany*
[3]*University of Wisconsin Milwaukee, 3135 N Maryland Ave, Milwaukee, WI 53211, USA*

We present the first atlas of the continuous gravitational wave sky, produced using LIGO O3a public data. For each 0.045 Hz frequency band and every point on the sky the atlas provides upper limits, signal-to-noise ratios (SNR) and frequencies where the search measures the maximum SNR. The results presented in the atlas are produced with the Falcon pipeline and cover nearly monochromatic gravitational wave signals in the 500-1000 Hz band, with up to $\pm 5 \times 10^{-11}$ Hz/s frequency derivative. Compared to the most sensitive results previously published (also produced with the Falcon pipeline) our upper limits are 50% more constraining. Neutron stars with ellipticity of 10^{-8} can be detected up to 150 pc away, while allowing for a large fraction of the stars' energy to be lost through non-gravitational channels.

I. INTRODUCTION

Continuous gravitational waves are expected from a variety of natural sources. Binaries of compact objects like white dwarves, neutron stars and black holes in a tight orbit are expected to emit continuous gravitational waves in the $10^{-3} - 10^{-1}$ Hz region – a region accessible to LISA[1]. Higher frequency continuous gravitational waves are produced by equatorially deformed rotating neutron stars and can be observed with ground-based laser interferometer observatories.

The amplitude of gravitational waves produced by deformed rotating neutron stars is proportional to the square of the rotational frequency and to their "*ellipticity*" - a measure of the equatorial deformation [2]. The strongest signals are thus produced by highly deformed fast-rotating objects.

Searches for continuous gravitational waves target known pulsars using rotation-frequency measurements from the radio, X- and gamma-ray observations [3–7], promising regions in the sky [8, 9], and unknown objects in all-sky surveys [10–15].

For broad searches over weeks of data or longer, a broad variety of approaches is used because the most sensitive methods cannot be used due to computational limitations. In these cases one has to sacrifice breadth of search or sensitivity or both. Our loosely coherent algorithms [16–18] and, in particular, the Falcon search pipeline [10–12] that is used for the analysis presented here, has performed very well in this trade-off.

Here we present the results of our search of LIGO public O3a data [19] for continuous gravitational wave signals with frequency between $\simeq$ 500 and 1000 Hz. Compared to our earlier analyses on O2 data i) we search a spin-down range larger by a factor $\gtrsim$ 16. This provides a larger margin ($\times 2.9$ at 1000 Hz) for Doppler shifts due to stellar motion and energy loss due to magnetic fields ii)

we use the more sensitive O3a data set iii) we provide a frequency-resolved atlas of the sky [20], i.e. upper limits on the gravitational wave intrinsic strain h_0 and measured signal-to-noise ratios (SNR) as a function of signal frequency and source sky-position.

The atlas provides sky-resolved data for every 45 mHz signal-frequency band. The sky resolution increases linearly with frequency, and at 1000 Hz for any point on the sky there is a grid point within a 0.26° radius. For each sky pixel and atlas frequency bin (45 mHz) we provide a 95% confidence level upper limits on the strain of continuous wave gravitational wave signals. The upper limits reported in the atlas are maximized over frequency in each 45 mHz bin, over nearby sky positions and over source orientation. The upper limits at the native resolution are obtained from the gravitational wave power values through the application of the universal statistic [21]. We also provide the maximum SNR value and the corresponding frequency. Our simulations show that if the maximum SNR exceeds 9, the signal frequency is within 0.6 mHz of the frequency of the maximum, with 95% confidence.

The atlas contains nearly two billion records. To make it accessible to a wider community, the atlas has been designed so that it can be analyzed on a small personal computer using the MVL library [22, 23]. We provide software that produces sky maps for wide frequency bands and allows queries of the atlas by sky position and/or frequency, and computations using the full scan of the data. Effectively this enables arbitrary searches within the covered parameter space with the full sensitivity of the Falcon pipeline, but without the need for a large computing cluster.

II. THE SEARCH

This search uses data of the LIGO H1 and L1 interferometers, from the publicly released O3a set [19]. We limit our search to the LIGO detectors because no other detector comes within a factor of 2 of their sensitivity.

The O3a data set is known to be contaminated by

---
[a] vladimir.dergachev@aei.mpg.de
[b] maria.alessandra.papa@aei.mpg.de

loud short-duration excesses of noise [14, 24]. To address this, we first prepare short Hann-windowed Fourier transforms (SFTs) with $0.25\,\mathrm{s}$ duration. We then monitor the frequency band 20-36 Hz for power excess that indicates noise contamination and exclude the affected SFTs from analysis. The remaining SFTs are searched with the Falcon pipeline.

We search for nearly monochromatic signals of the IT2 type [11], whose instantaneous frequency in the source frame at time t takes the form

$$f(t) = f_0 + (t - t_0)f_1 + (t - t_0)^2 f_2/2, \qquad (1)$$

where f_0 is the signal frequency at GPS epoch $t_0 = 1246070000$, and f_1 and f_2 are the linear and quadratic frequency drifts, respectively.

The search targets emission in the $500 - 1000\,\mathrm{Hz}$ frequency range, covering frequency derivatives $|f_1| \leq 5 \times 10^{-11}\,\mathrm{Hz/s}$ and $|f_2| \leq 4 \times 10^{-20}\,\mathrm{Hz/s^2}$.

Stage	Coherence length (days)	Minimum SNR
1	0.5	6
2	1	8
3	2	8
4	6	12

TABLE I. Parameters for each stage of the search. Stage 4 refines outlier parameters by using a denser sampling of parameter space, and then subjects them to an additional consistency check based on the analyses of individual interferometer data. Only the first two stages are used to construct atlas; stages 3 and 4 are solely outlier follow-ups.

The pipeline employs 4 stages (Table I) with coherence length increasing from 12 hours to 6 days. Results exceeding the SNR threshold of one stage pass to the next stage. The upper limits and the atlas are constructed based on the results of the first two stages only. This simplifies the upper limit procedure without significant impact on the sensitivity. The last stage of the pipeline has sufficient sensitivity to see signals in data from individual interferometers and hence signal consistency checks can be performed by comparing results from each detector.

III. RESULTS

Five outliers survive all stages (Table II): Three correspond to simulated signals injected via radiation pressure on the detectors' test masses (Table III). One is induced by a large instrumental artifact in H1. One outlier with SNR just above threshold, does not correspond to any identifiable detector artifact, however a reanalysis of this outlier using public data from the O3a and O3b [25] LIGO runs combined yields a decrease in the SNR below 13. This is not consistent with what is expected from the IT2 continuous signal model (Eqn. 1) assumed in this search.
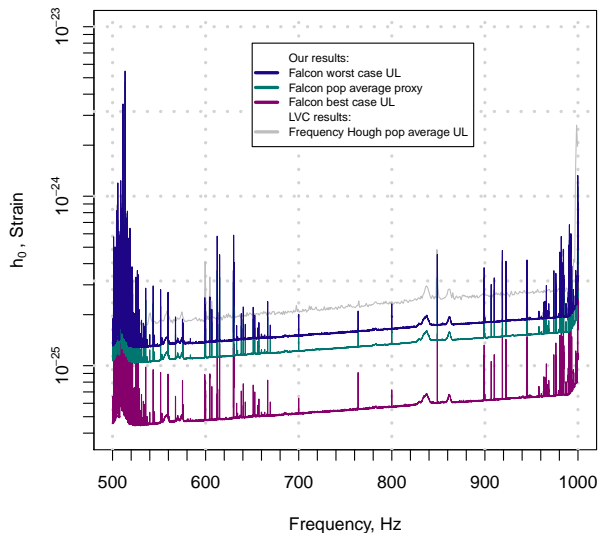

FIG. 1. Gravitational wave intrinsic amplitude h_0 upper limits at 95% confidence as a function of signal frequency. The upper limits are a measure of the sensitivity of the search. We introduce a "population average" proxy upper limit in order to compare with the latest LIGO/Virgo all-sky results [15]. In this frequency range [15] are a factor $\gtrsim 1.65$ less constraining than ours, albeit able to detect sources with much higher deformations.

Based on the search results we compute upper limits on the intrinsic amplitude h_0 of continuous gravitational waveforms as a function of signal frequency and source sky position. In particular, in the atlas we provide upper limits maximized over all polarizations and for circularly polarized signals alone. The upper limits from the atlas are summarized in Figures 1 and 2, which are produced by taking the maximum over the sky in each 45 mHz bin. This is the traditional way to present continuous wave upper limit results.

The upper limits can be taken as a measure of the sensitivity of our search, and recast in terms of the ellipticity ε of sources that the search is able to detect:

$$\varepsilon = \frac{c^4}{4\pi^2 G} \frac{h_0 d}{I_{zz} f_0^2}, \qquad (2)$$

where I_{zz} is the moment of inertia of the star with respect to the principal axis aligned with the rotation axis and d its distance. This search is sensitive to sources with ellipticity of 10^{-8} up to 150 pc away, improving on our O2 results by a factor of ≈ 1.5 and on the full O3 results of [15] by a factor of ≈ 1.7. Signals sourced by ellipticities of 10^{-7} would have been detected from sources within a distance between 500 pc and 1.5 kpc, depending on the orientation, at the highest frequencies, or between 200 pc and 600 pc at the lowest frequencies.

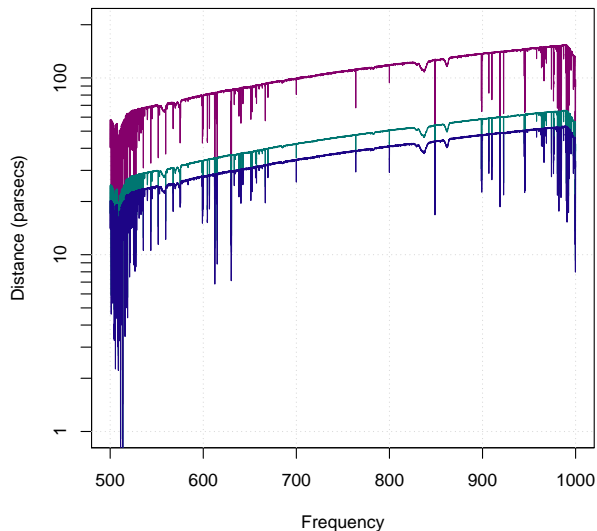A counterpart of our atlas is produced by the radiome-

FIG. 2. Reach of the search for stars with ellipticity of 10^{-8}. The search is also sensitive to sources with ellipticities of 10^{-7} with a distance from Earth that is 10 times higher. The X axis is the gravitational wave frequency, which is twice the pulsar rotation frequency for emission due to an equatorial ellipticity. R-modes and other emission mechanisms give rise to emission at different frequencies. The top curve (purple) shows the reach for a population of circularly polarized sources; The middle curve (cyan) holds for a population of sources with random orientations; The bottom curve (blue) holds for linearly polarized sources.

ter search for the gravitational wave stochastic background [26]. Both the radiometer and this search are affected by loud continuous signals. However, this search is specifically tuned to continuous signals as it, for example, tracks the signal Doppler shifts due to the Earth motion over months of observation. This makes it significantly more sensitive to continuous waves – and also more computationally expensive – than the radiometer search.

All-sky surveys for continuous gravitational waves are extremely computationally intensive: the results of this search cost in excess of 36 million CPU-hours. Our atlas [20] will allow others to benefit from this investment: astronomical observations of pulsations from a certain location in the sky may be checked against high SNR occurrences at the same location and consistent frequencies; the atlas can immediately be scanned across the whole frequency range at an interesting sky position, for example that of a supernova remnant, in search of a significant result; with an estimate of the distance of a gravitational wave source, upper limits on its ellipticity can be readily computed; models of neutron star populations can be directly convolved with the atlas upper limits to make predictions of their detectability, and the

same holds for primordial black hole populations emitting continuous gravitational waves through their orbital energy loss, or for tens of solar mass black hole populations sourcing continuous waves through super-radiance. The fine granularity of our atlas (Figures 3 and 4) produces high-number statistics and allows to estimate the significance of any finding.
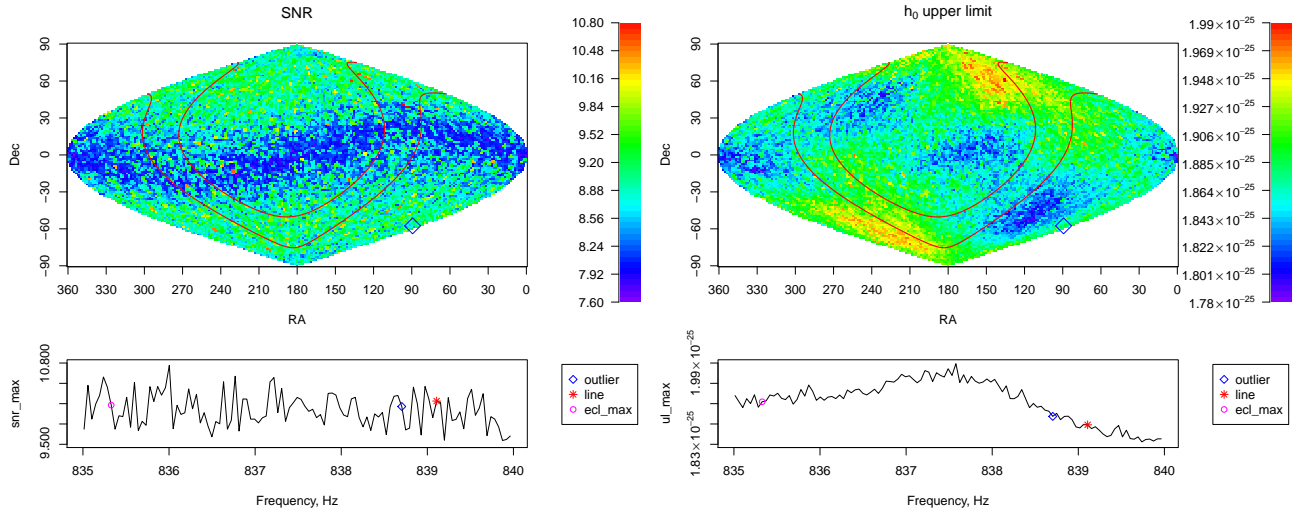
FIG. 3. Summary of atlas data from the bins between 835-840 Hz. The top panels show the highest SNR (left) and upper limit values (right) across the frequency band, for each pixel of the sky map, using equatorial coordinates. The red lines denote the galactic plane. The blue diamond shows the location of the outlier that is discarded based on the analysis of O3a+b data. The blue band of smaller SNRs near the ecliptic equator is due to large correlations between waveforms of sources in that region. The blue regions in the upper limit plot are due to the lower-SNR values in the ecliptic plane, and also occur near the ecliptic poles that are favored by the antenna pattern of the detectors. The bottom panels show the same data as a function of frequency and with the maximum taken over the sky. We mark the frequency of the band where the outlier mentioned above was found, the location of the only known line from the O3 line list in that band, and the band where we the maximum SNR is achieved in the ecliptic pole region - a region strongly affected by instrumental lines. The data and code used to produce this plot is available [20].

SNR	f	$\dot{f}$	RA$_{\text{J2000}}$	DEC$_{\text{J2000}}$	Comment
	Hz	pHz/s	degrees	degrees	
110.4	763.84732	−0.4	198.886	75.689	Simulated signal ip9
98.9	575.16351	−0.4	215.255	3.441	Simulated signal ip2
16.7	993.38180	7.0	282.198	−57.533	Line in H1
16.3	848.91931	−31.6	39.087	−15.706	Simulated signal ip1
16.1	838.70499	1.2	10.883	−57.581	Fails O3a+b consistency check

TABLE II. Outliers surviving the detection pipeline. Outliers marked "ipX" are due to simulated signals "hardware-injected" during the science run for validation purposes. Their parameters are listed in Table III. The outlier marked as "line" is close in frequency to a strong narrowband disturbance. Signal frequencies refer to GPS epoch 1246070000.

Label	h_0	Frequency	Spindown	RA$_{\text{J2000}}$	DEC$_{\text{J2000}}$
	10^{-25}	Hz	pHz/s	degrees	degrees
ip1	5.5	848.935	-300	37.39	-29.45
ip2	0.76	575.164	-0.137	215.26	3.44
ip9	1.3	763.847	-1.45×10^{-5}	198.89	75.69

TABLE III. Parameters of the hardware-injected simulated continuous wave signals during the O3 data run (epoch GPS 1246070000), that fall in the parameter range probed by our search.

[1] S. A. Hughes, "A Brief survey of LISA sources and science," AIP Conf. Proc. **873**, no.1, 13-20 (2006) doi:10.1063/1.2405017
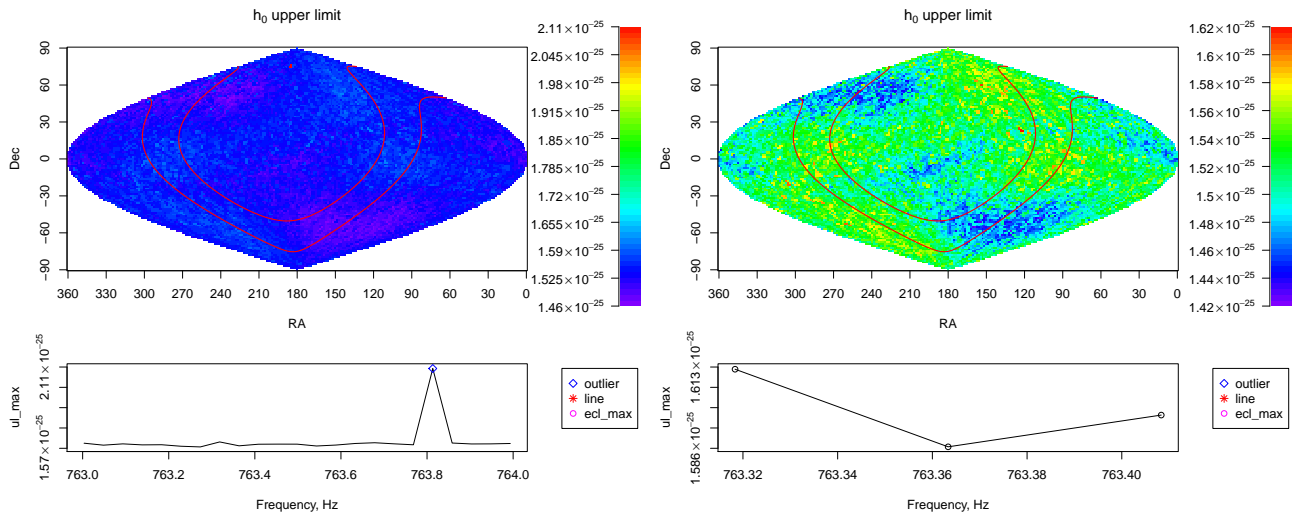
FIG. 4. Both panels here show upper limit results, like the right hand-side plots of Figure 3. The frequency band is different: 763-764 Hz for the left panels and a zoom between 763.3-763.42 for the right side panels. We choose the 763-764 band to give an idea of what a signal would like like, since the hardware-injected fake signal ip9 falls in this band, see Table III. The signal amplitude is 1.3×10^{-25} and it is lower than the upper limit value at the sky position, as it should be. The zoomed-in band does not contain the signal parameters and hence it is an example of a "quiet band".

[2] P. Jaranowski, A. Krolak and B. F. Schutz, "Data analysis of gravitational - wave signals from spinning neutron stars. 1. The Signal and its detection," Phys. Rev. D **58** (1998), 063001

[3] R. Abbott *et al.* [LIGO Scientific, VIRGO and KAGRA], "Searches for Gravitational Waves from Known Pulsars at Two Harmonics in the Second and Third LIGO-Virgo Observing Runs," [arXiv:2111.13106 [astro-ph.HE]].

[4] A. Ashok, B. Beheshtipour, M. A. Papa, P. C. C. Freire, B. Steltner, B. Machenschalk, O. Behnke, B. Allen and R. Prix, "New Searches for Continuous Gravitational Waves from Seven Fast Pulsars," Astrophys. J. **923**, no.1, 85 (2021) doi:10.3847/1538-4357/ac2582

[5] B. Rajbhandari, B. J. Owen, S. Caride and R. Inta, "First searches for gravitational waves from r-modes of the Crab pulsar," Phys. Rev. D **104**, no.12, 122008 (2021) doi:10.1103/PhysRevD.104.122008

[6] R. Abbott *et al.* [LIGO Scientific, Virgo and KAGRA], "Constraints from LIGO O3 Data on Gravitational-wave Emission Due to R-modes in the Glitching Pulsar PSR J0537–6910," Astrophys. J. **922**, no.1, 71 (2021) doi:10.3847/1538-4357/ac0d52

[7] L. Fesik and M. A. Papa, "First Search for r-mode Gravitational Waves from PSR J0537–6910," Astrophys. J. **895**, no.1, 11 (2020) [erratum: Astrophys. J. **897**, no.2, 185 (2020)] doi:10.3847/1538-4357/ab8193

[8] J. Ming, M. A. Papa, H. B. Eggenstein, B. Machenschalk, B. Steltner, R. Prix, B. Allen and O. Behnke, "Results From an Einstein@Home Search for Continuous Gravitational Waves From G347.3 at Low Frequencies in LIGO O2 Data," Astrophys. J. **925**, no.1, 8 (2022) doi:10.3847/1538-4357/ac35cb

[9] R. Abbott *et al.* [LIGO Scientific, VIRGO, KAGRA and Virgo], "Searches for Continuous Gravitational Waves from Young Supernova Remnants in the Early Third Observing Run of Advanced LIGO and Virgo," Astrophys.

J. **921**, no.1, 80 (2021) doi:10.3847/1538-4357/ac17ea

[10] V. Dergachev, M. A. Papa, "Results from the first all-sky search for continuous gravitational waves from small-ellipticity sources", Phys. Rev. Lett. **125**, no.17, 171101 (2020)

[11] V. Dergachev, M. A. Papa, "Results from high-frequency all-sky search for continuous gravitational waves from small-ellipticity sources", Phys. Rev. **D** 103, 063019 (2021)

[12] V. Dergachev, M. A. Papa, "The search for continuous gravitational waves from small-ellipticity sources at low frequencies", Phys. Rev. **D** 104, 043003 (2021)

[13] B. Steltner, M. A. Papa, H. B. Eggenstein, B. Allen, V. Dergachev, R. Prix, B. Machenschalk, S. Walsh, S. J. Zhu and S. Kwang, "Einstein@Home All-sky Search for Continuous Gravitational Waves in LIGO O2 Public Data," Astrophys. J. **909**, no.1, 79 (2021) doi:10.3847/1538-4357/abc7c9

[14] R. Abbot *et al.*(LIGO Scientific Collaboration, Virgo Collaboration and KAGRA Collaboration), "All-sky search for continuous gravitational waves from isolated neutron stars in the early O3 LIGO data",Phys. Rev. **D** 104, 082004 (2021)

[15] R. Abbot *et al.*(LIGO Scientific Collaboration, Virgo Collaboration and KAGRA Collaboration), All-sky search for continuous gravitational waves from isolated neutron stars using Advanced LIGO and Advanced Virgo O3 data, arXiv:2201.00697

[16] V. Dergachev, On blind searches for noise dominated signals: a loosely coherent approach, Class. Quantum Grav. **27**, 205017 (2010).

[17] V. Dergachev, Loosely coherent searches for sets of well-modeled signals, Phys. Rev. D **85**, 062003 (2012)

[18] V. Dergachev, Loosely coherent searches for medium scale coherence lengths, arXiv:1807.02351

[19] The O3a Data Release `https://doi.org/10.7935/`

`nfnt-hm34`

[20] See EPAPS Document No. [number will be inserted by publisher] for numerical values of upper limits. Also at `https://www.aei.mpg.de/continuouswaves/O3aFalcon500-1000` including full atlas.

[21] V. Dergachev, A Novel Universal Statistic for Computing Upper Limits in Ill-behaved Background, Phys. Rev. D **87**, 062001 (2013).

[22] Mappable Vector Library, `https://github.com/volodya31415/libMVL`

[23] R package for Mappable Vector Library `https://cran.r-project.org/package=RMVL`

[24] B. Steltner, M. A. Papa and H. B. Eggenstein, "Identification and removal of non-Gaussian noise transients for gravitational-wave searches," Phys. Rev. D **105**, no.2, 022005 (2022) doi:10.1103/PhysRevD.105.022005

[25] The O3b Data Release `https://doi.org/10.7935/pr1e-j706`

[26] R. Abbott *et al.* [LIGO Scientific, VIRGO and KAGRA], "All-sky, all-frequency directional search for persistent gravitational-waves from Advanced LIGO's and Advanced Virgo's first three observing runs," [arXiv:2110.09834 [gr-qc]].